AIP | Journal of Applied Physics

Direct measurement of pyroelectric figures of merit of proper and improper ferroelectrics

A. Shaulov, M. I. Bell, and W. A. Smith

Citation: J. Appl. Phys. 50, 4942 (1979); doi: 10.1063/1.325569
View online: http://dx.doi.org/10.1063/1.325569
View Table of Contents: http://jap.aip.org/resource/1/JAPIAU/v50/i7
Published by the American Institute of Physics.

Related Articles

Electro-caloric effect in 0.45BaZr0.2Ti0.8O3-0.55Ba0.7Ca0.3TiO3 single crystal
Appl. Phys. Lett. 102, 082902 (2013)

Interferometric measurement of the pyroelectric coefficient in lithium niobate
J. Appl. Phys. 113, 043101 (2013)

Dielectric and enhanced pyroelectric properties of (Pb0.325Sr0.675)TiO3 ceramics under direct current bias field
Appl. Phys. Lett. 101, 262901 (2012)

The study of dielectric, pyroelectric and piezoelectric properties on hot pressed PZT-PMN systems
AIP Advances 2, 042170 (2012)

Contribution of an extrinsic mechanism for the electrical polarization in BiMn2O5 ceramics
AIP Advances 2, 042165 (2012)

Additional information on J. Appl. Phys.

Journal Homepage: http://jap.aip.org/
Journal Information: http://jap.aip.org/about/about_the_journal
Top downloads: http://jap.aip.org/features/most_downloaded
Information for Authors: http://jap.aip.org/authors

ADVERTISEMENT

Downloaded 03 Mar 2013 to 132.70.33.156. Redistribution subject to AIP license or copyright; see http://jap.aip.org/about/rights_and_permissions

Transverse-acoustoelectric-voltage (TAV) spectroscopy of high-resistivity GaAs[a)]

H. Estrada-Vazquez, R. T. Webster, and P. Das

Electrical and Systems Engineering Department, Rensselaer Polytechnic Institute, Troy, New York 12181
(Received 28 March 1978; accepted for publication 6 March 1979)

The space-charge-coupled interaction of surface acoustic waves (SAW) propagating on a piezolectric substrate with a semiconductor surface placed in proximity gives rise to a transverse acoustoelectric voltage. This voltage is developed across the semiconductor and is dependent on the semiconductor surface conductivity. Thus, the spectral response of the acoustoelectric voltage gives information about the interaction of impurity and defect levels of the semiconductors with the conduction and valence bands. Maxima and minima in the photoenhanced acoustoelectric voltage are due to corresponding structures in the photoconductivity. Experimental results on semi-insulating gallium arsenide with no intentional doping, Cr doping, and Cr-Te doping are reported. The results include the dependence of the acoustoelectric voltage on light intensity and on temperature. Peaks in the spectral response are interpreted as impurity levels. Thus, a sharp peak at 0.87 eV is attributed to Cr-level–to–conduction-band transitions and the broad peak centered about 0.72 eV is attributed to oxygen impurities. The absorption threshold determines the Fermi-level location in the energy band and this, in turn, determines the sample resistivity. The experimental temperature dependence of band-gap energy agrees with previously reported results. Photocurrent measurements were also performed and a remarkable correlation between the two spectra was obtained. An important advantage of the TAV technique is the fact that it is contactless, nondestructuve, and requires no special preparation.

PACS numbers: 78.20.Hp, 72.50. + b

I. INTRODUCTION

High-resistivity GaAs plays an important role in the solid-state-device development, i.e., microwave devices and semiconductor lasers. Using oxygen[1] and/or chromium[2] as deep-level impurities in GaAs, high resistivity can be achieved. Due to the greater reproducibility obtained by Cr doping, this element has become the more often-used alternative for this purpose.

Compensation of the shallow energy-level impurities by Cr and/or O is considered to be the mechanism for reduction in free carriers. Several models have been proposed to explain the electrical properties of deep-level compensated GaAs.[3] Since the high resistivity of semiconductors and many other interesting effects (e.g., infrared photoluminescence) are due to the presence of these deep centers, the characterization of these are of great interest. This semiconductor impurity-level characterization can be performed by several powerful techniques such as DLTS (deep-level transient spectroscopy),[4] photomagnetoelectric effect,[5] photocapacitance,[6] photoluminescense,[7] photoabsorption,[8] photoconductivity,[9,10] optical transient-current spectroscopy,[11] and the photo-Hall effect.[5,9] However, some of the abovementioned techniques are not suitable for high-resistivity materials.

Recently, a technique[12–15] has been developed to do semiconductor surface spectroscopy using surface acoustic waves (SAW). This technique has the distinct advantage of requiring no Ohmic contact and thus it is highly suitable for high-resistivity materials. The purpose of this paper is to discuss the use of this technique in the study of deep levels in semi-insulating GaAs.

The SAW is excited by an interdigital transducer fabricated directly on the surface of a piezoelectric crystal. The mechanical motions are confined to the surface of the crystal, decaying exponentially within the crystal away from the surface. The mechanical vibrations are accompanied by a propagating electric field which exists both inside and outside the crystal. When a semiconductor sample is placed in the proximity of a SAW delay line, this electric field penetrates the semiconductor and interacts with the carriers near

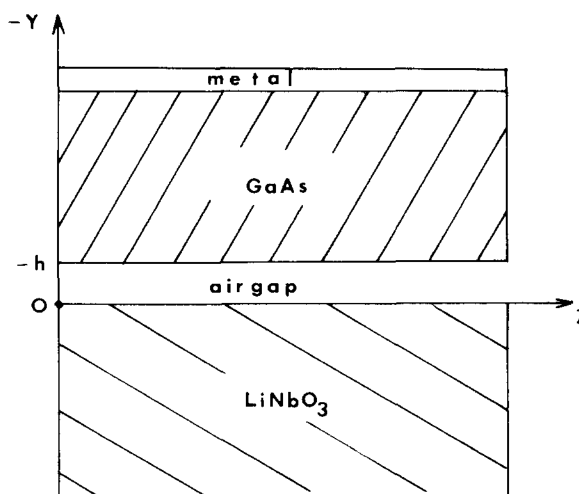

FIG. 1. Geometry of the test structure.

 © 1979 American Institute of Physics

Downloaded 03 Mar 2013 to 132.70.33.156. Redistribution subject to AIP license or copyright; see http://jap.aip.org/about/rights_and_permissions

the semiconductor surface. The geometry of the structure is illustrated in Fig. 1. The surface acoustic wave is excited on the piezoelectric substrate by an interdigital transducer. The frequency of the transducer is determined by the finger spacing and the SAW velocity. The surface acoustic wave can be described as a linear combination of terms of the form[16]

$$U = \sum_{i=1}^{4} U_i \exp(\alpha_i ky) \exp[j(\omega t - kz)], \quad y>0, \quad (1)$$

$$\phi = \sum_{i=1}^{4} \phi_i \exp(\alpha_i ky) \exp[j(\omega t - kz)], \quad y<0, \quad (2a)$$

or

$$\phi = \phi_0 \exp(-ky) \exp[j(\omega t - kz)], \quad y<0, \quad (2b)$$

where U is the particle displacement, ϕ is the electric potential, α is a dimensional decay constant, ω is the angular frequency, k is the wave number, and y and z are defined in Fig. 1. Particular values of U_i, α_i, and α_i are determined from the boundary conditions. While the particle motion is of course confined to the piezoelectric crystal ($y>0$), the electric potential exists both inside and outside the crystal. The decay constant of the electric potential outside the crystal ($y<0$) depends upon the electrical boundary conditions in that region. When the piezoelectric is bounded by free space, the electric-potential-field decay constant is the acoustic wavelength as shown in Eq. (2b).

When a semiconductor sample is positioned near the delay-line surface and separated from it by a uniform gap, the electric field associated with the SAW will penetrate the semiconductor. The potential ϕ of Eq. (2) will also depend upon the electrical characteristics of the semiconductor. In addition, the carrier concentrations of the semiconductor will be perturbed from their equilibrium values by the electric potential associated with the propagating SAW. The interaction of the excess carriers with this potential is the source of the acoustoelectric voltage. The component in the y direction (transverse with respect to the SAW propagation direction) can be detected by metal plates placed below the delay line and above the semiconductor and is called transverse acoustoelectric voltage (TAV).

The dependence of TAV on semiconductor conductivity can be illustrated by the simplifying assumption of an extrinsic semiconductor with negligible carrier recombination. The following expressions for the electric potential ϕ inside the semiconductor can be obtained in terms of the semiconductor parameters[17]:

$$\phi(y,z) = \exp[j(\omega t - kz)] \sum_{i=1}^{4} A_i \exp(\alpha_i ky), \quad (3)$$

where

$$\alpha_i = 1, -1, \alpha, -\alpha,$$

$$\alpha^2 = \left(1 + \frac{\omega_C \omega_D}{\omega^2} + j\frac{\omega_D}{\omega}\right),$$

and where $\omega_C = \sigma/\epsilon_s$, the dielectric relaxation frequency; $\omega_D = v_s^2/D$, the diffusion frequency; v_s is the SAW velocity on piezoelectric materials, ϵ_s is the semiconductor dielectric constant; D is the semiconductor diffusion constant; and σ is the conductivity. The values of A_i are found from the boundary conditions. Assuming the semiconductor thickness is much greater than a wavelength requires A_i to be zero for negative α_i's since the potential must be zero for large negative y. Thus the potential is given be the sum of two terms, one with a decay constant of the acoustic wavelength and the other with a decay constant of α. For frequencies of interest $\omega \gg \omega_D$ and for extrinsic semiconductors, $\alpha \gg 1$. Therefore, for an n-type semiconductor α can be approximated by

$$\alpha \approx \left(\frac{\omega_{Cn}\omega_{Dn}}{\omega^2}\right)^{1/2} = \frac{1}{k}\left(\frac{qn}{\epsilon_s k_B T}\right)^{1/2} = \frac{1}{k\lambda_D}, \quad (4)$$

where n is the concentration of free electrons, k_B is Boltzmann's constant, T is the temperature, q is the electronic charge, and λ_D is the effective Debye length. Quantities subscripted with n refer to electrons while those with p subscripts refer to holes. Thus the potential field decays within the semiconductor with a decay constant of the shorter of the effective Debye length λ_D and the acoustic wavelength λ. Using electrostatic approximations and solving the appropriate boundary-value equations, an expression for the TAV can be derived.[17] The result is

$$V_{\mathrm{TAV}} = V_0 \frac{n\mu_n - p\mu_p}{n\mu_n + p\mu_p} \times \frac{\omega R_2}{\omega^2 R_2^2(1+\epsilon_p/\epsilon_s)^2 + (\gamma + \epsilon_p/\epsilon_s)^2}, \quad (5)$$

where

$$R_2 = \frac{\omega_{Cn}\omega_{Dn}^2 + \omega_{Cp}\omega_{Dp}^2}{(\omega_{Cn}\omega_{Dn} + \omega_{Cp}\omega_{Dp})^2}\gamma,$$

$$\gamma^2 = 1 + \frac{\omega_{Cn}\omega_{Dn} + \omega_{Cp}\omega_{Dp}}{\omega^2},$$

and where n is the electron concentration, p is the hole concentration, μ_n is the electron mobility, μ_p is the hole mobility, ϵ_p is the dielectric constant of the piezoelectric material, and V_0 is a constant incorporating acoustic power, temperature, piezoelectric coupling coefficient, and frequency.

In Fig. 2 the TAV of Eq. (5) is plotted as a function of carrier concentration in GaAs. Thermal equilibrium is assumed, that is, $np = n_i^2$, where n_i is the intrinsic carrier concentration. The TAV tends to zero for both high and low carrier concentration, while it reaches a maximum at some intermediate value. The TAV is positive for n-type semiconductors and negative for p-type semiconductors.

This simple case demonstrates the general features of the transverse acoustoelectric voltage. A more complete model would include carrier lifetime, air gap thickness, semiconductor surface potential, surface recombination velocity, and finite semiconductor thickness. A theory including these parameters will be published separately.[17]

Using the conductivity dependence of the acoustoelectric voltage described above, TAV spectroscopy can be performed. The spectroscopy consists of monitoring the transverse component of the acoustoelectric voltage when the GaAs samples are irradiated with monochromatic light. The

Downloaded 03 Mar 2013 to 132.70.33.156. Redistribution subject to AIP license or copyright; see http://jap.aip.org/about/rights_and_permissions

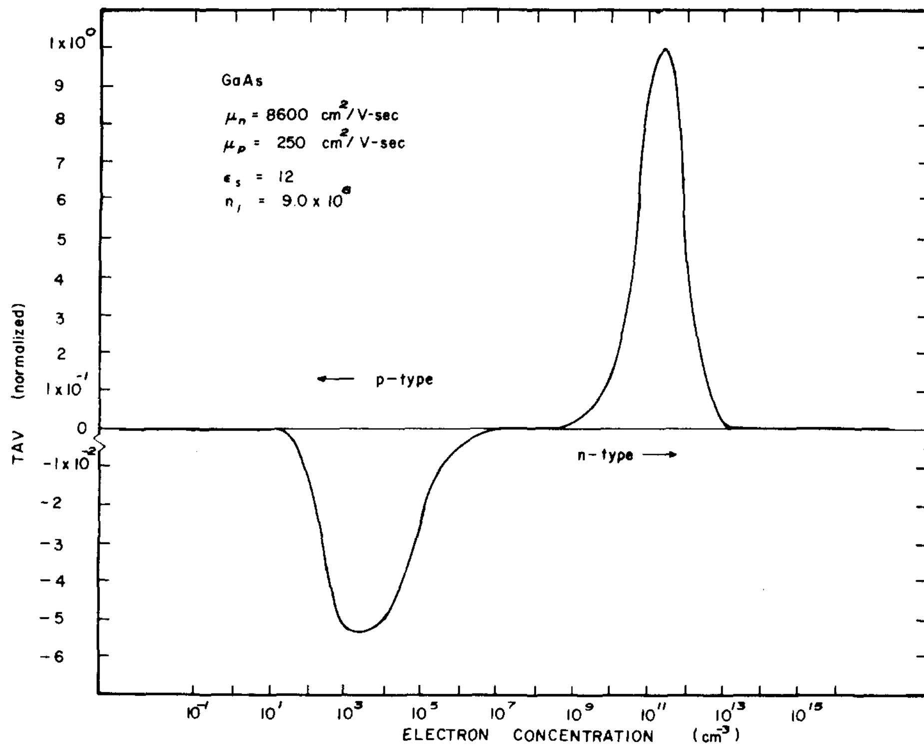

FIG. 2. Plot of the dependence of TAV for GaAs on carrier concentration obtained from Eq. (5).

absorption of photons produces transitions of electrons from filled to empty states. But only the transitions which change the free-carrier concentration of the semiconductor sample are detected by the acoustoelectric voltage. The dependence of the polarity of the TAV on carrier type aids in identifying the particular transition responsible for the maxima and minima in the TAV spectral response. This technique is a simple and sensitive nondestructive test since neither mechanical nor electrical contact of the surface being studied is required.

In Sec. II, the experimental procedure used in TAV spectroscopy is described. This is followed by the experimental results and discussion in Sec. III.

II. EXPERIMENTAL TECHNIQUES

The setup used in TAV spectroscopy is shown in Fig. 3, where the main device is the SAW convolver. Terminals 1 and 2, which are the input-output of the SAW delay line, are two interdigital transducers used to generate and detect the surface wave on the piezoelectric substrate (YZ-$LiNbO_3$). The TAV is measured at terminal 3. The operating frequency of these transducers is 45 MHz, which corresponds to a SAW wavelength of about 80 μm. The acoustic aperture of the transducers is $\sim$2.5 mm and the propagation direction for the acoustic waves is the Z axis of the crystal. rf-modulated pulses from 1 to 10-msec duration and 12-V peak-to-peak amplitude were applied to the input transducer.

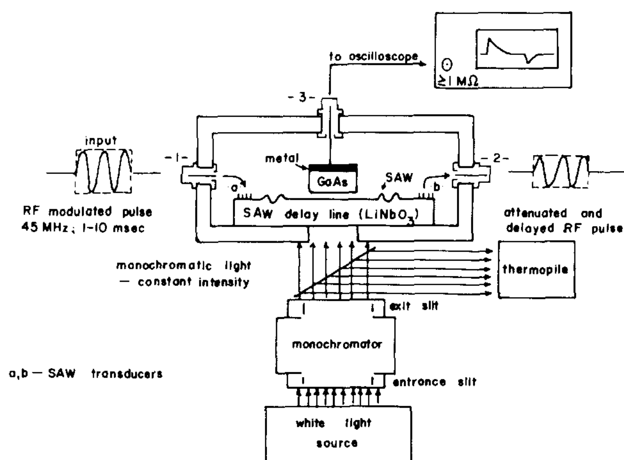

FIG. 3. Experimental setup for TAV spectroscopy where the main device is a SAW convolver.

The semiconductor samples, cut from wafers obtained from different manufacturers, are described in Table I. Their approximate dimensions are 4×6 mm and about 0.3–0.5 mm thick. Caution was taken to avoid organic contamination by cleaning the samples with TCE-acetone and deionized water before their study. Silver paint was used as the metallic backcontact for the semiconductor. These samples were illuminated uniformly with monochromatic light provided by a Bausch and Lomb High-Intensity monochromator; the light intensity was monitored with a thermopile detector and controlled constant by means of the entrance slit of the monochromator. Five different filters and three grat-

TABLE I. High-resistivity GaAs samples used in this study.

Sample designation	Source	Dopants	Properties (Ω cm)
A	NRL	"None"	$\rho > 10^7$
B	Laser Diodes Inc.	Cr	$\rho = 1.1\times 10^6$
C	NRL	Cr, Te Cr$\sim 3\times 10^{16}$ cm^{-3} Te$\sim 1\times 10^{16}$ cm^{-3}	$\rho > 10^7$

Downloaded 03 Mar 2013 to 132.70.33.156. Redistribution subject to AIP license or copyright; see http://jap.aip.org/about/rights_and_permissions

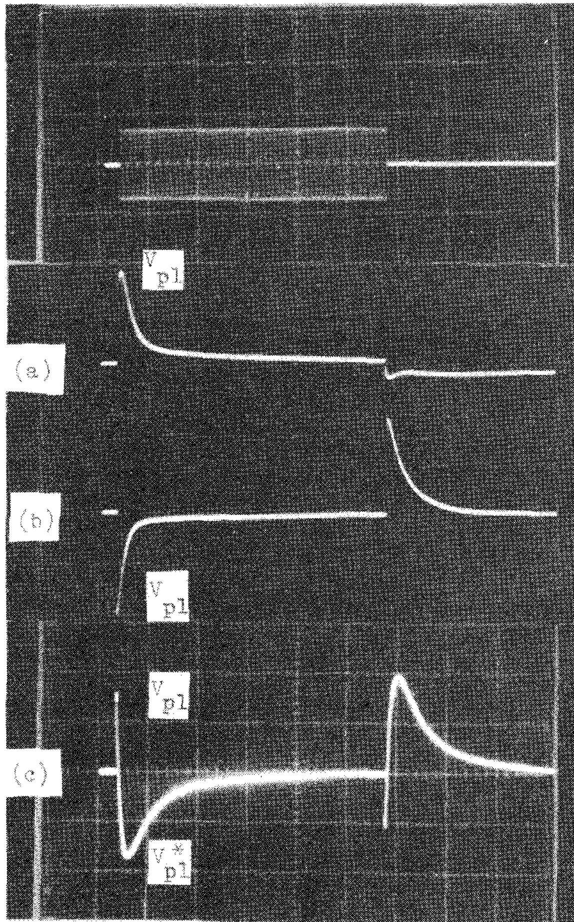

FIG. 4. Observed waveforms of the transverse acoustoelectric voltage. (a) and (b) are the waveforms for n- and p-type semiconductors, respectively, in dark conditions; this waveform has been labeled type A; (c) waveform shown by GaAs when irradiated with light of certain energies (type B). Vertical scale arbitrary: horizontal scale: 0.5 msec/div.

ings were used to cover the wavelength spectrum of interest [4000–20 000 Å (3.1–0.62 eV)]. The resolution of the light beam was better than 100 Å in the whole range, i.e., less than 0.05 eV in all the experiments. Caution was taken to assure constant illumination throughout the range, and calibrations of the transmittance spectrum for the $LiNbO_3$ samples were performed. The transmittance of the material is nearly constant in this range of wavelengths.

For TAV measurements below 300 °K the samples were mounted in an exchange-gas cooled Dewar. A thermoresistance was placed in one of the corners of the SAW convolver box to monitor the temperature. The window of this box was aligned to the Dewar's window so that semiconductor samples were uniformly illuminated. With this apparatus TAV was easily measured at any fixed temperature between 80 and 300 °K.

Typical waveforms of TAV are shown in Fig. 4. The TAV can be observed only as a transient phenomenon due to the absence of a dc path in the test structure. The TAV charges the capacitances associated with the structure and with the semiconductor surface which causes the measured output to decay toward zero. The time constant of the decay depends on the impedance of the external circuitry and on the dynamics of the population and depopulation of the defect states. When the acoustic wave is removed, the source of the acoustoelectric voltage is also removed causing the output voltage to invert and decay again to zero owing to the discharging of the capacitances. The waveforms of Figs. 4(a) and 4(b) correspond to n- and p-type semiconductors, respectively. In the TAV spectra the initial peak, labeled V_{p1} in Fig. 4, is plotted as a function of photon energy. A more complex waveform, Fig. 4(c), is observed when the incident radiation has photon energy near the value of band-to-band transition and near strong photoconductivity peaks. This is also found in CdS and is qualitatively explained considering the nonlinear interaction discussed in Ref. 15 when this phe-

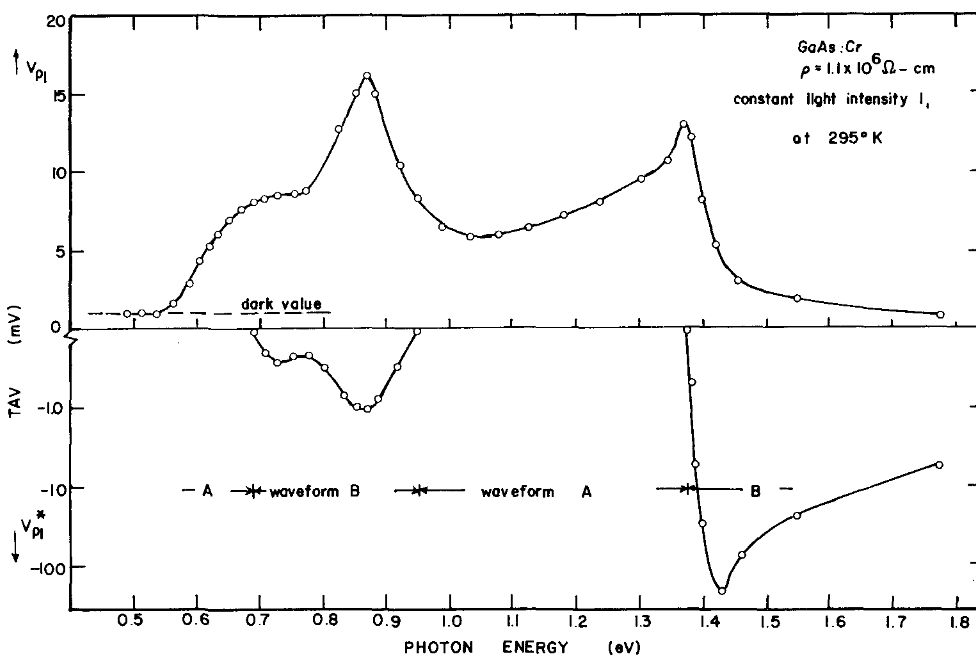

FIG. 5. TAV spectral response of GaAs : Cr at room temperature and constant light intensity I_1. Peak values of V_{p1} are plotted. The plot at the bottom shows peak values of V_{p1}^* in log scale when waveform B is observed.

Downloaded 03 Mar 2013 to 132.70.33.156. Redistribution subject to AIP license or copyright; see http://jap.aip.org/about/rights_and_permissions

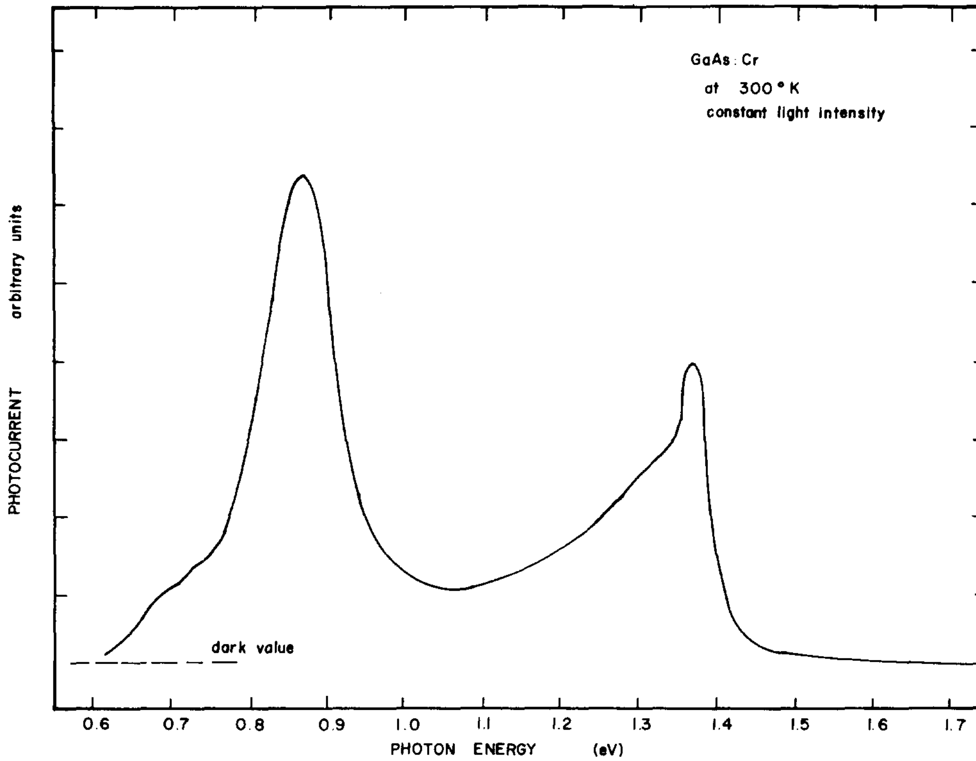

FIG. 6. Photocurrent spectroscopy of GaAs : Cr.

nomenon occurs. The negative peak value is labeled V_{pl}^{*}. The surface photocurrent for different wavelengths of incident light were also measured using a Kiethley picoammeter. Two metallic contacts with silver paint were used for this purpose. The photocurrent was measured both with and without applied constant bias voltage. The results obtained show no significant change in the shape of the curve except for the magnitude of the photocurrent.

III. EXPERIMENTAL RESULTS AND DISCUSSION

Experimental results for Cr-doped GaAs are presented in Figs. 5–9. TAV spectral response of GaAs : Cr : Te is shown in Fig. 10. Figures 11–14 present the results obtained from the undoped samples. Careful analysis of these figures points out the following properties of GaAs, especially the impurity levels in the energy-band diagram as shown in Fig. 15.

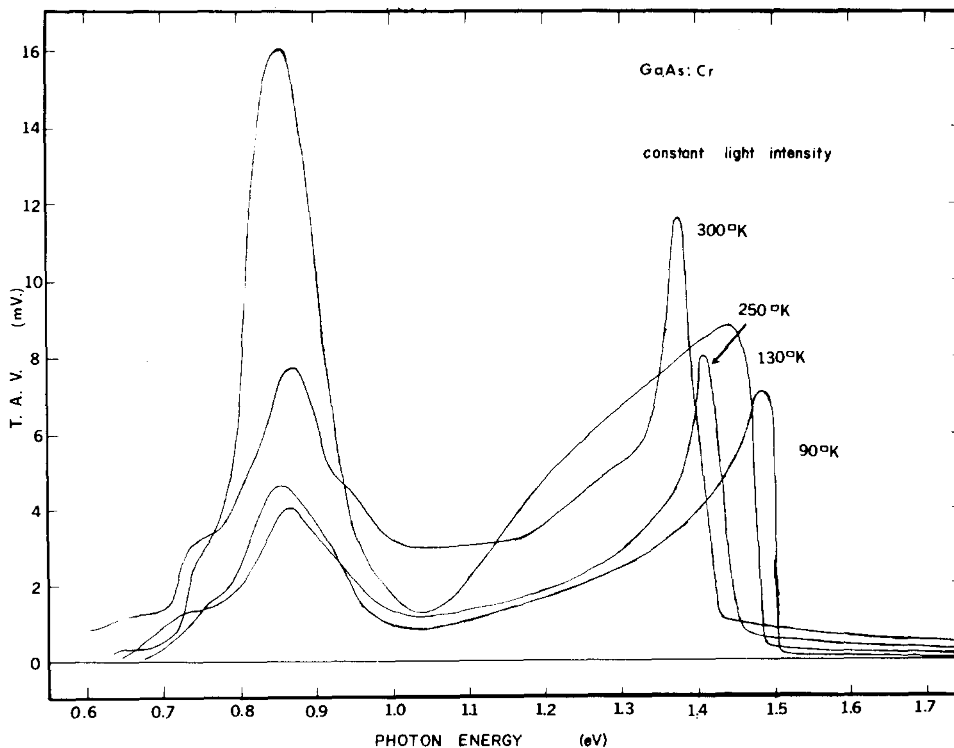

FIG. 7. TAV spectroscopy of GaAs : Cr at different temperatures and constant light intensity. Peak values of V_{pl} are plotted.

Downloaded 03 Mar 2013 to 132.70.33.156. Redistribution subject to AIP license or copyright; see http://jap.aip.org/about/rights_and_permissions

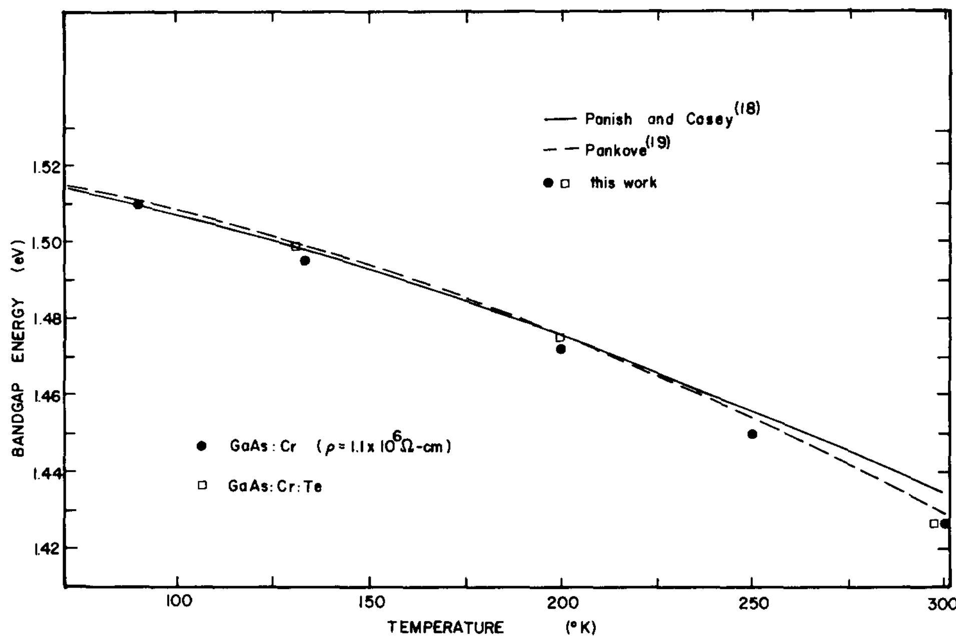

FIG. 8. Energy band gap of GaAs as a function of temperature obtained from the TAV spectral response shown in Fig. 7. Solid and dashed lines show previously reported data for comparison.

(a) The band-gap illumination at 1.43 eV produces a minimum in all the measured spectra at room temperature. The position of this minimum is found to be a function of temperature as shown in Fig. 7. A plot of these experimental band-gap-energy–versus–temperature points shown in Fig. 8 is in excellent agreement with other reported results.[18,19] For photon energies slightly lower than band gap, a large peak is observed in all spectra. In GaAs : Cr : Te, this peak around 1.42 eV is found to have a double hump indicating the presence of a Te level near the conduction band. However, the resolution of the monochromator is not sufficient to obtain any quantitative information.

(b) The Cr level at 0.87 eV from the conduction band[20] also produces a large peak in the spectral response. However, the position of this peak is found to be rather insensitive to temperature. The magnitude of the peak does have a maximum at 130 °K. This might be due to a maximum in mobility at this temperature.

(c) A comparison of the GaAs : Cr photocurrent spectra of Fig. 6 with the corresponding room-temperature TAV spectra Fig. 7 shows reasonable agreement. Both exhibit large peaks near 0.87 eV and near 1.4 eV. Similarly, the undoped GaAs photocurrent spectra of Fig. 12 compares well with the 1-mW/cm^2 TAV spectra of Fig. 13. These comparisons indicate that the TAV is, in fact, detecting photoinduced changes in conductivity.

(d) Although the dominant structures are around 1.43 and 0.87 eV, there are other structures observed in the spec-

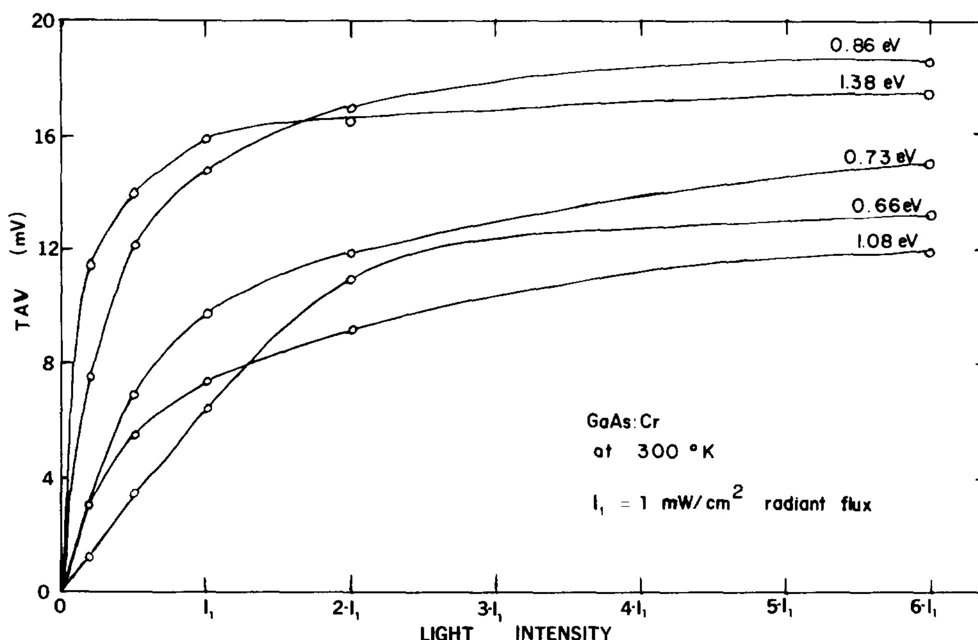

FIG. 9. Dependence of GaAs : Cr TAV on the illumination intensity of different photon energies.

Downloaded 03 Mar 2013 to 132.70.33.156. Redistribution subject to AIP license or copyright; see http://jap.aip.org/about/rights_and_permissions

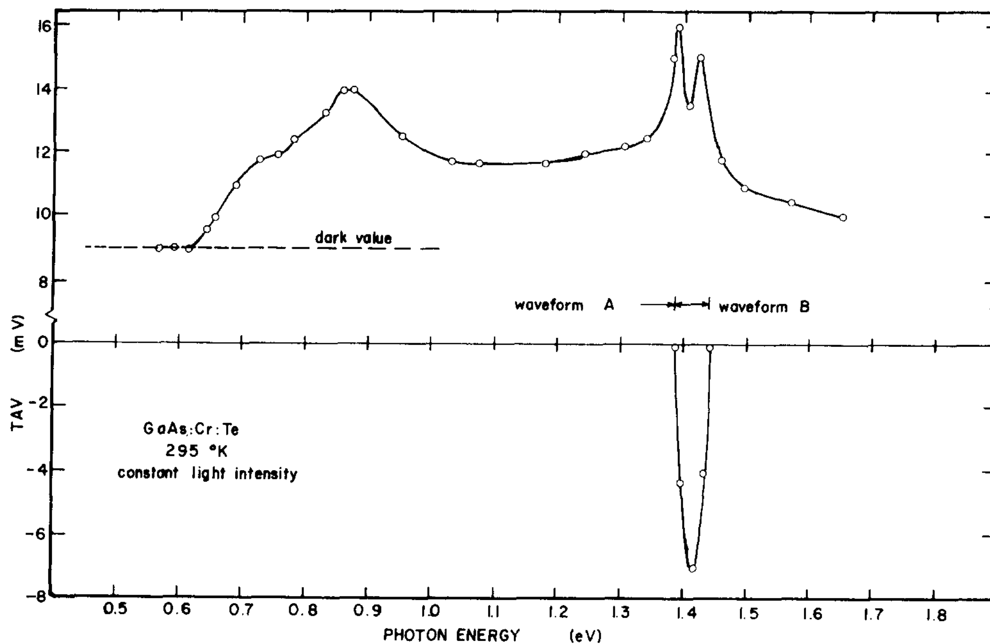

FIG. 10. TAV spectral response of GaAs : Cr : Te at room temperature and constant light intensity. Peak values of V_{p1} are plotted. The plot at the bottom corresponds to V_{p1}^* when waveform B is observed.

tral responses around 0.69 eV for all samples, and around 0.9 and 1.2 eV for undoped samples. The 0.69-eV level can be associated with the presence of an oxygen level.[3,9,21]

(e) The measured dark values of the acoustoelectric voltage described in Sec. II showed that all the samples are n type. Their resistivities can be estimated if we interpret the threshold of the TAV photoresponse as the carrier transition of minimum energy; this establishes an approximate position of the Fermi level. Good correlation of the threshold values with the sample resistivity is observed; samples with greater conductivity will show higher Fermi levels. The observed threshold values of extrinsic excitations occur at 0.557, 0.605, and 0.620 eV for samples B, A, and C, respectively.

We get the sample resistivity ρ by using the well-known equations

$$n = N_C \exp[-(E_C - E_F)/kT]$$

and

$$p = N_V \exp[-(E_F - E_V)/kT]$$

for the density of electrons and holes, respectively, and

$$\rho = (qn\mu_n + qp\mu_p)^{-1}$$

for the sample resistivity, where $N_C = 2(2\pi m_e^* k_B T/h^2)^{3/2}$ is the density of states in the conduction band, $N_V = 2(2\pi m_h^* k_B T/h^2)^{3/2}$ is the density of states in the va-

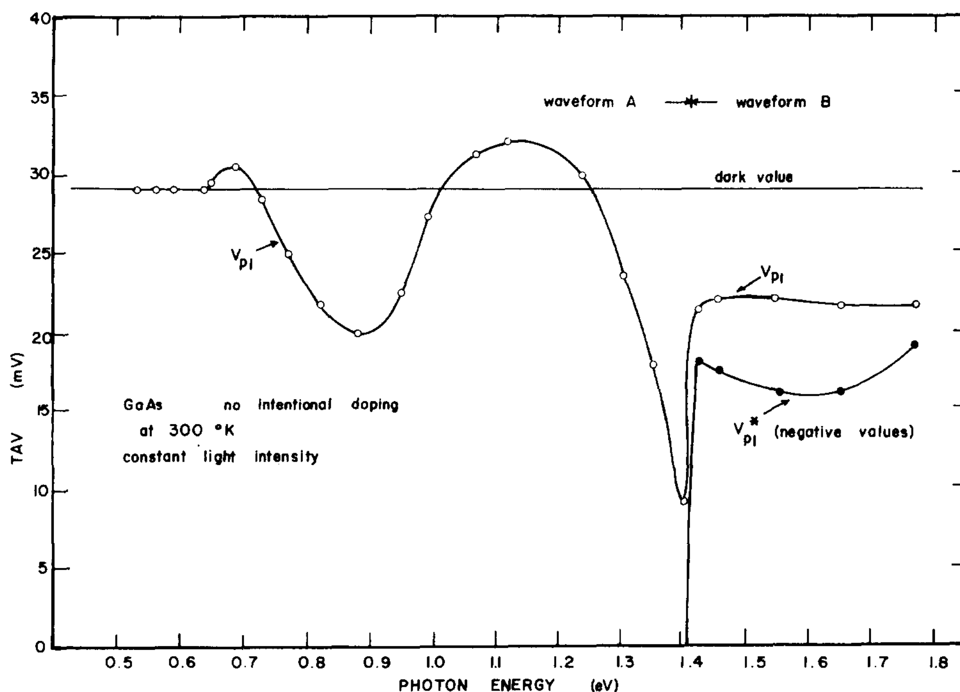

FIG. 11. TAV spectral response of undoped GaAs at room temperature and constant light intensity. Plot shows peak values of V_{p1} and V_{p1}^*. V_{p1}^* has negative values, see Fig. 4.

Downloaded 03 Mar 2013 to 132.70.33.156. Redistribution subject to AIP license or copyright; see http://jap.aip.org/about/rights_and_permissions

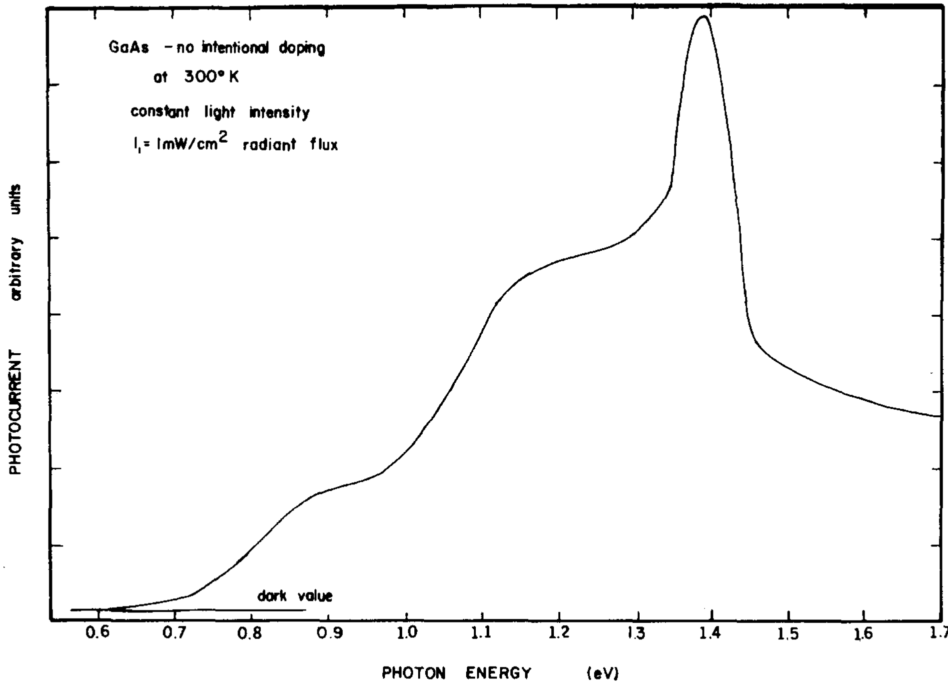

FIG. 12. Photocurrent spectroscopy of undoped GaAs.

lence band, m_e^* and m_h^* are the effective masses of electrons and holes, respectively, and q is the elementary charge. E_c is the conduction band energy, E_V is the valence-band energy, h is Planck's constant, and T is the absolute temperature. By using $\mu_n = 8500$ cm^2/V sec and $\mu_p = 400$ cm^2/V sec, we get the following values for the resistivities: ρ(sample B) $= 3.15 \times 10^6$ Ω cm, ρ(sample A)–2.0×10^7 Ω cm, and ρ(sample C) $= 3.5 \times 10^7$ Ω cm, which correlate very well with the information provided by the manufacturers: 1.1×10^6 Ω cm for sample B and resistivities greater than 10^7 Ω cm for samples A and C.

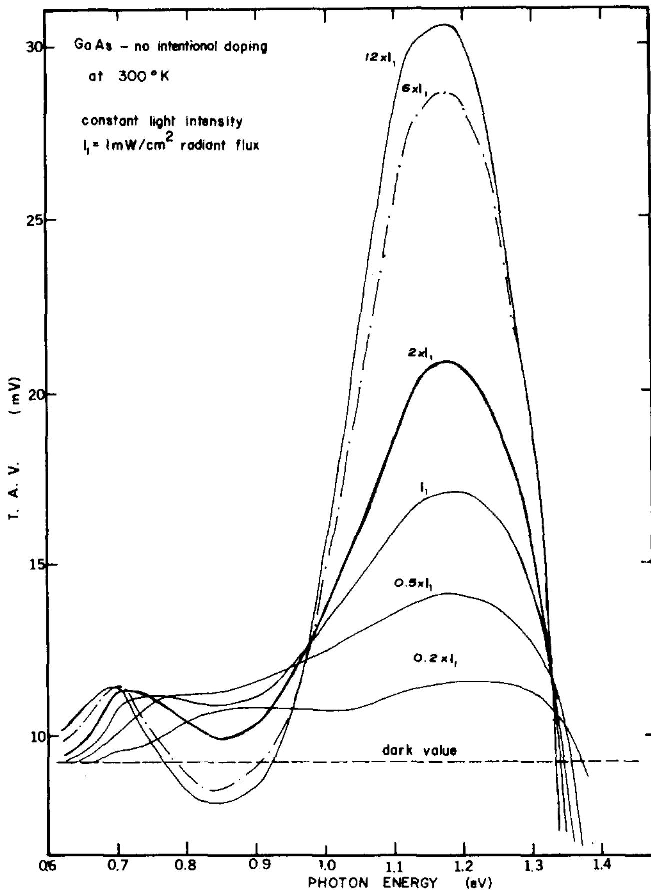

FIG. 13. TAV spectral response of undoped GaAs at different light intensities.

(f) The photoconductivity is a nonlinear function of the light intensity.[22] This nonlinearity should also be reflected in the light-intensity dependence of TAV which is shown in Fig. 9 for GaAs : Cr. It is found that in general the TAV saturates at high intensity although the saturation value and the rate of approach to saturation depend on the wavelength. The intensity dependence of undoped GaAs shown in Figs. 13 and 14 is found to be more complex. For example, at 0.87 eV, the TAV increases initially, reaches a maximum, and then decreases. This decrease can be attributed to the change in conductivity due to hole-generating transitions because the TAV due to holes has opposite polarity to that due to electrons. The strong monotonic dependence of the light intensity around 1.2 eV (Fig. 13) indicates the position of either an unknown impurity level or surface states. This is also indicated by a plateau in the photocurrent spectral response of Fig. 12. It has been reported that electron traps in GaAs have been detected at 0.98, 1.18, and 1.21 eV by using the thermal stimulated conductivity technique[9] and at 1.12, 1.27, and 1.35 eV using the transient capacitance spectroscopy technique.[23] The contributions of these traps to the acoustoelectric voltage may be responsible for the behavior discussed here.

(g) It is pointed out that the slow photoresponse (~ 10 min) was observed in the acoustoelectric voltage for all samples studied here. It is well known[22] that the slowness in the growth of photoconductivity is a direct result of trapping.

Downloaded 03 Mar 2013 to 132.70.33.156. Redistribution subject to AIP license or copyright; see http://jap.aip.org/about/rights_and_permissions

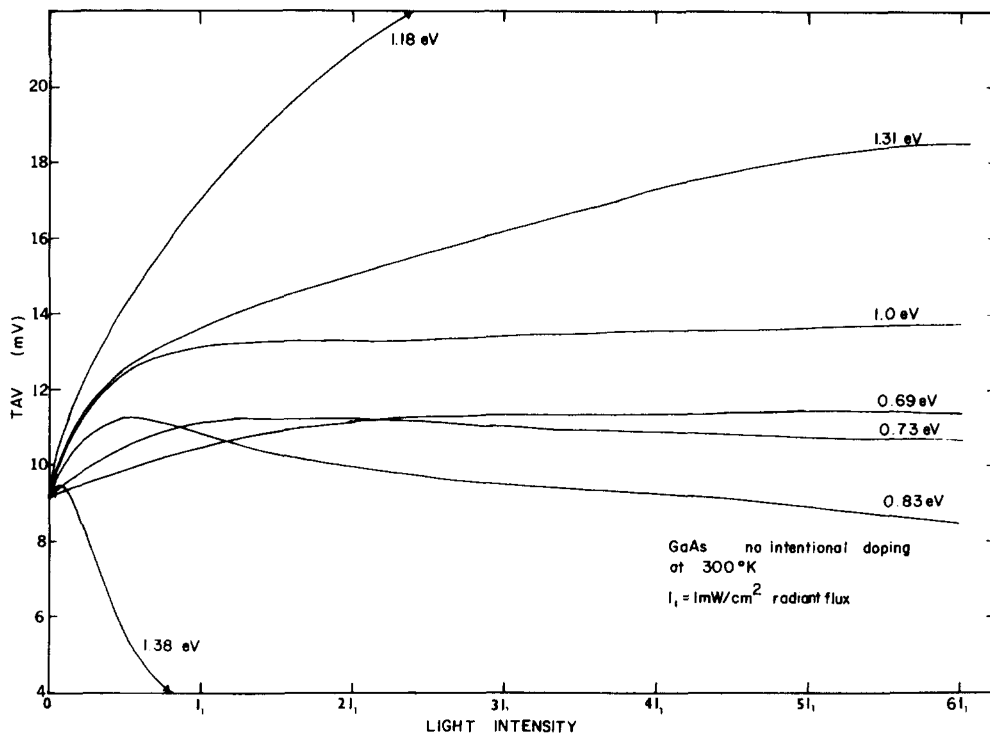

FIG. 14. Dependence of undoped GaAs TAV on the illumination intensity of different photon energies.

Carriers excited to the conduction band when the sample is initially illuminated will be almost immediately trapped, such that some time is required to reach steady-state sample conductivity when low-intensity excitation is taking place. These traps lie between the conduction band and Fermi level, but lying rather closer to the latter so that thermal excitation is not possible. Slowness in the photoconductivity decay when illumination is turned off is also due to the effect of traps. The emptying of these deep traps dominates and controls the decay.

The analysis of the experimental results as presented above is somewhat qualitative except for the positions of levels in the energy-band diagram. To obtain any quantitative results, one should obtain a theoretical expression for TAV as a function of quasi-Fermi level which in turn can be related to the incident radiation. This work is presently being pursued.

In summary, a SAW technique has been used to perform the spectroscopy of GaAs samples. Extensive measurements have been performed and good correlation with photocurrent data has been obtained.

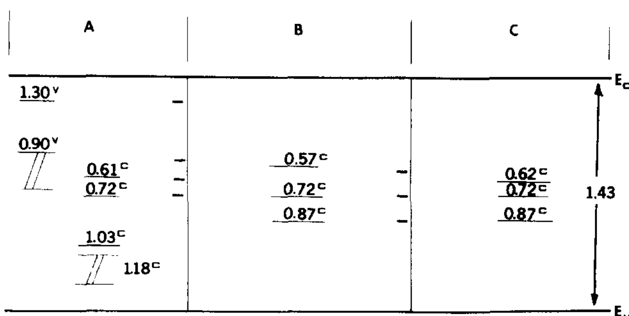

FIG. 15. Energy-band diagram of GaAs showing positions of impurity levels.

ACKNOWLEDGMENTS

The authors would like to thank Dr. E. Swiggard of the Naval Research Laboratory for supplying GaAs material, Professor J. Borrego for his helpful discussions, and Dr. M. K. Roy for generating the plot of Fig. 2.

[1] J. Blanc and L. R. Weisberg, Nature **192**, 155 (1961).
[2] G. R. Cronin and R. W. Haisty, J. Electroch. Soc. **111**, 874 (1964).
[3] R. Zucca, J. Appl. Phys. **48**, 1987 (1974).
[4] D. V. Lang, J. Appl. Phys. **45**, 3023 (1974).
[5] D. C. Look, J. Electron. Mater. **147** (1978).
[6] A. M. White, P. Porteous, and P. J. Dean, J. Electron. Mater. **5**, 91 (1978).
[7] M. Schmidt and H. J. Stocker, J. Appl. Phys. **49**, 4438 (1978).
[8] D. Bois and P. Pinard, Phys. Rev. B **9**, 4171 (1974).
[9] A. L. Lin and R. H. Bube, J. Appl. Phys. **47**, 1859 (1976).
[10] H. J. Stocker, J. Appl. Phys. **48**, 4583 (1977).
[11] C. Hurtes, M. Boulou, A. Mittonneau, and D. Bois, Appl. Phys. Lett. **32**, 821 (1978).
[12] P. Das, M. E. Motamedi, and R. T. Webster, Appl. Phys. Lett. **27**, 120 (1975).
[13] P. Das, M. E. Motamedi, and R. T. Webster, Solid-State Electron. **19**, 121 (1976).
[14] P. Das, M. E. Motamedi, H. Gilboa, and R. T. Webster, J. Vac. Sci. Technol. **13**, 948 (1976).
[15] H. Gilboa and P. Das, Surface Sci. **62**, 536 (1977).
[16] *Surface Wave Filters*, edited by H. Matthew (Wiley, New York, 1977), p. 55.
[17] H. Gilboa and P. Das (unpublished); Technical Report No. MA-ONR-15, Office of Naval Research Contract No. N00014-75-C-0772, 1977.
[18] M. B. Panish and H. C. Casey, Jr., J. Appl. Phys. **40**, 163 (1969).
[19] J. I. Pankove, *Optical Processes in Semiconductors* (Dover, New York, 1971), p. 412.
[20] W. H. Koschel, S. G. Bishop, and B. D. McCombe, Bull. Am. Phys. Soc. **21**, 251 (1976).
[21] A. G. Milnes, *Deep Impurities in Semiconductors* (Wiley, New York, 1973), p. 48.
[22] R. H. Bube, *Photoconductivity in Solids* (Wiley, New York, 1960), Chap. 9, p. 273.
[23] D. V. Lang, R. A. Logan, and L. C. Kimerling, Proc. of the 13th Intern. Conference on Physics of Semiconductors, 1976, p. 615 (unpublished).

Downloaded 03 Mar 2013 to 132.70.33.156. Redistribution subject to AIP license or copyright; see http://jap.aip.org/about/rights_and_permissions